Sol-gel synthesis of tantalum oxide and phosphonic acid-modified carbon nanotubes composite coatings on titanium surfaces

Maho, Anthony; Detriche, Simon; Delhalle, Joseph; Mekhalif, Zineb

Published in:
Materials Science & Engineering C

DOI:
10.1016/j.msec.2013.02.025

Publication date:
2013

Document Version
Peer reviewed version

Sol-gel synthesis of tantalum oxide and phosphonic acid-modified carbon nanotubes composite coatings on titanium surfaces

Anthony Maho[a,b], Simon Detriche[a], Joseph Delhalle[a], Zineb Mekhalif[a,*]

[a] Laboratory of Chemistry and Electrochemistry of Surfaces, University of Namur (FUNDP), Rue de Bruxelles 61, B-5000 Namur, Belgium. E-mail: zineb.mekhalif@fundp.ac.be

[b] Fonds pour la Formation à la Recherche dans l'Industrie et dans l'Agriculture (FRIA), Rue d'Egmont 5, B-1000 Bruxelles, Belgium.

Abstract

Carbon nanotubes used as fillers in composite materials are more and more appreciated for the outstanding range of accessible properties and functionalities they generate in numerous domains of nanotechnologies. In the framework of biological and medical sciences, and particularly for orthopedic applications and devices (prostheses, implants, surgical instruments, …), titanium substrates covered by tantalum oxide/carbon nanotubes composite coatings have proved to constitute interesting and successful platforms for the conception of solid and biocompatible biomaterials inducing the osseous regeneration processes (hydroxyapatite growth, osteoblasts attachment). This paper describes an original strategy for the conception of resistant and homogeneous tantalum oxide/carbon nanotubes layers on titanium through the introduction of carbon nanotubes functionalized by phosphonic acid moieties (-P(=O)$(OH)_2$). Strong covalent C-P bonds are specifically inserted on their external sidewalls with a ratio of two phosphonic groups per anchoring point. Experimental results highlight the stronger "tantalum capture agent" effect of phosphonic-modified nanotubes during the sol-gel formation process of the deposits comparing to nanotubes bearing oxidized functions (-OH, -C=O, -C(=O)OH). Particular attention is also paid to the relative impact of the rate of functionalization and the dispersion degree of the carbon nanotubes in the coatings, as well as their wrapping level by the tantalum oxide matrix material. The resulting effect on the *in vitro* growth of hydroxyapatite is also evaluated to confirm the primary osseous bioactivity of those materials. Chemical, structural and morphological features of the different composite deposits described herein are assessed by X-ray photoelectron spectroscopy (XPS), scanning (SEM) and transmission (TEM) electronic microscopies, energy dispersive X-rays analysis (EDX) and peeling tests.

Keywords

Titanium; Tantalum oxide; Carbon nanotubes; Phosphonic acid; Sol-gel; Biomaterials.

Corresponding author

* Prof. Zineb Mekhalif, Laboratory of Chemistry and Electrochemistry of Surfaces, University of Namur (FUNDP), Rue de Bruxelles 61, B-5000 Namur, Belgium. Tel.: +32 (0)81 72 52 30. Fax: +32 (0)81 72 46 00. E-mail: zineb.mekhalif@fundp.ac.be

1. Introduction

The use and impact of titanium (Ti) as bulk material in biomedical sciences has been increasingly investigated and developed those recent years. Thanks to their very interesting mechanical and biochemical properties (appropriate Young modulus and density, high solidity and fatigue strength, reinforced biocompatibility, inertness to human body, corrosion resistance, …), titanium-based biomaterials can be exploited for the design of various surgical instruments as well for the elaboration of cardiovascular, dental and osseous implants and prostheses [1-6]. However, the lack of strong bioactive properties – especially osseointegration abilities for orthopedic devices – combined with long-term degradation effects under physiological conditions and potential toxicity of alloying elements (nickel in Nitinol, vanadium in Ti-6Al-4V, …) require the development of specific solving strategies [7-12]. For this purpose, a successful approach based on the deposition of thin tantalum (Ta) layers on the titanium surfaces has been reported. Indeed, tantalum as coating material reinforces the biocompatibility and bioactivity features of the titanium platforms, while increasing their corrosion resistance and bringing them radio-opacity (interesting for medical imagery applications) [13-16].

In an attempt to globally strengthen the tantalum deposit (internal cohesion, adherence with the titanium surface), we intend to take advantage of the exceptional mechanical properties of multiwalled carbon nanotubes (MWCNTs) by incorporating them in so-called composite coatings [17]. Moreover, CNTs integrated into such layers are able to bio-mimic the collagen fibers structure (organic component of the osseous matrix), which can also specifically increase the interactions with osteoblasts and osteoclasts (osseous body cells) and favor hydroxyapatite (inorganic component of the osseous matrix) formation on the surface, which are the first steps of the integration process of a bone implant into the human body [18,19]. To this extent, the sol-gel co-deposition technique has been particularly praised for its practical easiness and its use of non-expensive materials [20-25].

From a general point of view, the main challenge for the design of high-quality composite biomedical devices based on CNTs lies in the control of their incorporation as reinforcements. A first key parameter involves thus the quality of their global wrapping by the matrix material (here Ta_2O_5). Several publications in the literature already focused their attention on this very particular aspect, and especially on the coating and/or filling of the CNTs with metal and metal oxide nanoparticles (NP) or nanolayers as matrix. For instance, Ma and Zhang reported the coverage of multiwalled carbon nanotubes (MWCNTs) by Au-NP for electrochemical sensing applications [26]. Tan *et al.* performed the preparation of magnetic nanocomposites by depositting γ-Fe_2O_3 nanoparticles on both inner and outer surfaces of MWCNTs [27], while Liu *et al.* managed to synthesize Fe_3O_4-MWCNTs nanocomposites [28]. Gao *et al.* succeeded for their part in covering MWCNTs with a 5-10 nm layer of TiO_2 through a surfactant wrapping sol-gel process, leading to high-performance

semi-conducting devices [29]. Recently, our group also managed to selectively and uniformly decorate MWCNTs with copper and nickel nanocrystals for energy-related purposes [30,31].

An important attention must also be paid to the quality of the CNTs dispersion into the matrix component of the composite. In many cases, this is achieved through the control of their dispersion in a solution-phase during the preparation process of the material, for which different approaches are described in the literature. Crude CNTs can be dispersed in an appropriated solvent, which is conveniently selected following the Hansen Solubility Parameters (HSPs) theory [32,33]. The use of well-chosen surfactants or additives can also be exploited, but those molecules are sometimes considered as impurities and cannot always be removed posteriorly from the material without losing a proper dispersion [34]. Ultimately, the possibility of a direct organic modification on the nanotubes sidewalls remains one of the best ways to achieve the projected dispersion, even if this method can partially damage the electrical and mechanical properties of the CNTs [34-41]. Several reactions leading to covalent functionalization of carbon nanotubes have been described: halogenation, cycloadditions, ozonolysis, nucleophilic and electrophilic additions, hydrogenation, … [34] The most common and practical approach generally involves the introduction, through strong oxidative treatments (typically nitric acid/sulfuric acid mixtures), of oxygen-containing functions (-OH, -C=O, -C(=O)OH), mainly at the level of defect sites on the tubes sidewalls. Furthermore, other chemical functionalities like acyl chlorides, esters, amides and phosphates can be produced on these alcohol and carboxyl groups [34-41].

In the context of the present work, our aim is to promote the formation of strong and homogeneous tantalum coatings on CNTs, a target we believe to be best achieved via the covalent attachment of phosphonic acid moieties (-P(=O)$(OH)_2$) to their outer surface. Phosphonic acids present a high affinity for many ions and elements, notably tantalum [42,43] and calcium, and are thus involved in numerous biochemical reactions and functions. Such compounds are increasingly used in medicine, especially as antibacterial, anticancer and anti-HIV agents, but also as therapeutic vectors for bone diseases [44]. In this framework, bisphosphonates molecules, with two phosphonic groups sharing a common carbon atom and forming a strong and resistant P-C-P bond, are particularly considered as powerful drugs for the treatment of osteoporosis and other osseous resorption disorders [45,46]. A few reports have already described the covalent introduction of phosphonic groups at the surface of CNTs by reacting 2-aminoethylphosphonic acid on carboxy-modified MWCNTs [47], binding diethyl (hydroxymethyl)phosphonate and diethyl (4-aminobenzyl)phosphonate on acyl chloride functions generated on carboxy-modified single-walled carbon nanotubes (SWCNTs) [48], or attaching aminopropyl-phoshonic acid on fluorinated SWCNTs [49]. In this work, we propose to covalently bind bisphosphonic acid groups on the carbon atoms present at the surface of MWCNTs in a direct procedure. The reaction involved has been reported by the groups of Lecouvey and Lecollinet: first acyl chloride functions are obtained by reacting carboxyl groups with thionyl chloride, then

tris(trimethylsilyl) phosphite is added to transform them into bisphosphonic acid functions [50,51]. This specific MWCNTs functionalization can be of significant importance knowing the high stability and resistance of carbon-to-phosphorus links toward chemical hydrolysis, thermal decomposition and photolysis in various media, including those exploited here for the sol-gel process [23,25,52,53]. Moreover, the specific introduction of two phosphonic groups per anchoring point appears as highly interesting and ingenious. To the best of our knowledge, such a direct introduction of strong covalent P-C-P bonds on the outer surface of carbon nanotubes has never been achieved and described previously. The methodology reported in this paper (Fig. 1) is simple and involves relatively mild practical conditions.

This paper describes the original synthesis of bisphosphonic acid-modified multiwalled carbon nanotubes (P-MWCNTs) and their incorporation through a sol-gel formation process in tantalum oxide composite coatings on titanium substrates. Attention is particularly paid to the effect of the modification treatment of the nanotubes in the efficiency of their integration into the deposits. The characteristics of the P-MWCNTs and the different composite layers are assessed by X-ray photoelectron spectroscopy (XPS), scanning (SEM) and transmission (TEM) electronic microscopies, energy dispersive X-rays analysis (EDX) and peeling tests. *In vitro* hydroxyapatite (HAp) growth tests are finally achieved to evaluate qualitatively the global impact of the different layers on the osseous bioactivity of the systems.

2. Materials and methods

2.1. Products and reagents

The following chemicals and solvents are used without further purification for the carbon nanotubes oxidation and sol-gel deposition processes: potassium permanganate (Merck), sulfuric acid (Chem-Lab NV, 95-97%), nitric acid (Aldrich, ≥65%), tantalum butoxide (Aldrich, 98%), hydrochloric acid (Chem-Lab NV, 37%), acetone (Chem-Lab, 99+%) and absolute ethanol (VWR Prolabo). Thionyl chloride (Sigma-Aldrich, 97%), hexane (dried on molecular sieves, Sigma-Aldrich, ≥95%), methanol (CHROMASOLV, ≥99.9%), tris(trimethylsilyl)phosphite (Aldrich, ≥95%) are employed as received for the functionalization reaction. Simulating body fluid (SBF) is prepared in ultra-pure water (18.2 MΩ cm) with the following salts: sodium chloride (Acros, 99.5%), potassium chloride (Aldrich, ≥99.0%), magnesium hexahydrate chloride (Acros, 99%), calcium dihydrate chloride (Merck, 99.5%), sodium hydrogenocarbonate (Acros, 99+%), potassium hydrogenophosphate (Acros, 99+%), sodium sulfate (Janssen Chimica, 99%) and tris(hydroxymethyl)aminomethane (Acros, 99.8%).

2.2. Titanium substrates preparation

Rectangular-shaped (15 mm x 10 mm) 1 mm thick titanium plates are used as substrates (Advent, 99.98%). Coupons are first mechanically polished on a Buehler-Phoenix 4000 instrument using a silicon carbide paper (P320) followed by a 9 µm diamond paste (Struers). They are then etched down to 0.02 µm using a 4/1 v/v mixture of colloidal silica polishing suspension (Buehler) and hydrogen peroxide (Fluka, 30%). Ti samples are then ultrasonically cleaned in absolute ethanol (15 min) and in acetone (15 min), and finally treated with UV-ozone for 15 min (Jelight 42-220) in order to eliminate all physisorbed contaminations prior to modification. A native oxide layer is formed during this process.

2.3. Treatments on multiwalled carbon nanotubes

2.3.1. Oxidized MWCNTs (O-MWCNTs)

0.5 g of MWNT 7000 carbon nanotubes (Nanocyl) are submitted to a specific oxidative treatment in a 0.1 M $KMnO_4/H_2SO_4$ mixture at 60°C during 2 h [25]. The obtained samples are washed with distilled water until a pH of 5 is obtained, and then submitted to a lyophilisation process.

2.3.2. Bisphosphonic acid-modified MWCNTs (P-MWCNTs)

A chemical pathway similar to the one reported by Lecouvey's and Lecollinet's groups has been used [50,51]. This two steps reaction consists first in the transformation of a carboxylic acid function into acyl chloride, followed by its conversion into a bisphosphonic acid group by the action of tris(trimethylsilyl) phosphite. In a typical experiment, 100 mg of previously oxidized CNTs (see below) are stirred at 60°C in 10 mL of thionyl chloride during 2 h, which

are then removed by distillation under vacuum. CNTs are redispersed in 20 mL of dry hexane and 500 µL of tris(trimethoxysilyl)phosphite are added slowly. This mixture is heated at 60°C for 2 h, followed by addition of 10 mL of methanol. After one night of stirring at room temperature, CNTs are filtered on Buchner and washed with acetone and pentane. Two kinds of P-MWCNTs have been prepared and used in this study: "weakly-modified" (*weak* P-MWCNTs) and "strongly-modified" (*strong* P-MWCNTs). The degree of functionalization by phosphonic groups is directly related to the intensity of the initial oxidative treatment of the CNTs in a H_2SO_4/HNO_3 3/1 v/v mixture (see below in *P-MWCNTs characterization* section): 2 h at 50°C for *weak* P-MWCNTs, 4 h at 60°C for *strong* P-MWCNTs.

2.4. Sol-gel co-deposition of tantalum oxide/MWCNTs composites

Sol-gel solution contains 4.0 mL of absolute ethanol, 0.2 mL of HCl as acid catalyst and 8.0 mg of MWCNTs (O-MWCNTs, *weak* P-MWCNTs or *strong* P-MWCNTs, depending of the cases). Carbon nanotubes are dispersed ultrasonically during 30 minutes, then 1.0 mL of $Ta(OBu)_5$ is added dropwise. The solution is kept under stirring for 2 h before use for the modification of mechanically and chemically polished titanium samples. After an immersion step of 10 min in the sol-gel solution, these are further submitted to a gradual hydrolysis in ultra-pure water during 10 min, and then dried at 300°C during 3 min (Fig. 2) [24,25]. Pristine Ta_2O_5 deposits are also prepared on Ti for the needs of comparison. In this case, $Ta(OBu)_5$ is directly introduced dropwise in the sol-gel solution, which is in this case absolutely free of CNTs.

2.5. Nucleation of hydroxyapatite

The hydroxyapatite formation on modified Ti samples is achieved by their immersion in 10 mL of a SBF for 7 days at 37°C. SBF solutions are prepared through the dissolution of NaCl, KCl, $MgCl_2.6H_2O$, $CaCl_2.2H_2O$, $NaHCO_3$, K_2HPO_4 and Na_2SO_4 in ultra-pure water, with the following ionic concentrations (in mM): Na^+ 142.0, K^+ 5.0, Mg^{2+} 1.5, Ca^{2+} 2.5, Cl^- 148.0, HCO_3^- 4.2, HPO_4^{2-} 1.0, and SO_4^{2-} 0.5 [7]. They are then buffered at pH 7.25 with tris(hydroxymethyl)aminomethane and 37% hydrochloric acid. The working SBF solution is renewed every 48 h to ensure the constancy of the ionic concentrations.

2.6. XPS characterization

X-ray photoelectron spectroscopy (XPS) is used to assess the elemental composition of the modified Ti samples. Spectra are measured on a Surface Science SSX-100 spectrometer. The photoelectrons are excited using a monochromatized Al Kα radiation as the excitation source, collected at 35° from the surface normal and detected with a hemispherical analyzer. The spot size of the XPS source on the sample is about 600 µm, and the analyzer is operated with a pass energy of 20 eV. Pressure is kept below (1×10^{-9} Torr) during data acquisition, and the binding energies of the obtained peaks is made with reference to the binding energy of the C1s line set at 285.0 eV, characteristic of the aliphatic carbons. Spectra are fitted using

a linear combination of Gaussian and Lorentzian profiles, with a Gaussian character let free to vary between 60 and 100%. Peak positions obtained after analysis are found essentially constant (± 0.3 eV). The different relative peak areas are finally estimated.

2.7. SEM and TEM imaging, EDX mapping and peeling tests procedures

A scanning electron microscopy (SEM) study is performed on a JEOL microscope 7500F to evaluate the morphological and structural characteristics of the Ta_2O_5 pristine and Ta_2O_5/MWCNTs composite coatings. The size and morphology of the hydroxyapatite crystals posteriorly formed on the substrates are also characterized, as well as their chemical composition thanks to an energy dispersive X-rays (EDX) analyzer. Wrapping of carbon nanotubes by Ta_2O_5 in the layers is evaluated by transmission electron microscopy (TEM) with a Phillips Tecnai 10 instrument. Peeling tests for adhesion evaluation of the tantalum-based deposits are carried out according to the ASTM D3359 protocol. Modified samples are scratched with a metallic comb with spacing streak of 1 mm (Electrometer 1542, ASTM D3359). A scotch tape is then stuck on the peeled surface and removed. SEM pictures of the scratched areas of the layer give a qualitative assessment of the adhesive nature of the coating.

3. Results and discussion

3.1. P-MWCNTs characterization

The principal issue of this work concerns the improvement of the incorporation capacities of MWCNTs in a Ta_2O_5 matrix for the formation of composite coatings at the surface of titanium plates. The proposed approach relies on a specific functionalization of the nanotubes outer surface with phosphonic acid ($–P(=O)(OH)_2$) functions, acting as "tantalum capture agents" during the sol-gel co-deposition process. Two kinds of P-MWCNTs are exploited in this paper: *weak* P-MWCNTs and *strong* P-MWCNTs (Fig. 1). Their main characteristics are briefly described in this section.

Fig. 3 represents the XPS survey spectra of *weak* P-MWCNTs (a) and *strong* P-MWCNTs (b). The nature of the modified nanotubes is assessed in both cases by the detection of C1s, O1s and P2p signals. Small contributions for Si (contamination from the adhesive tape used for the XPS experiments) and Al (catalyzer residues from the crude CNTs synthesis protocol) are also noticed. The nature of the phosphonic functionalization is confirmed by the binding energy value of 133.6 eV measured for the P2p peak with good reproducibility (on at least 3 samples). Concerning the experimental P/C ratios, they highlight the fact that more phosphonic functions are present on *strong* P-MWCNTs (P/C = 0.024) than on *weak* P-MWCNTs (P/C = 0.010). The yield of the MWCNTs modification reaction by phosphonic groups is thus directly dependent of the strength of their initial oxidative treatment.

3.2. Elaboration of Ta_2O_5/MWCNTs composite coatings on Ti: the direct impact of P-MWCNTs

In order to counterbalance the weaknesses of pure titanium as orthopedic bulk biomaterial (long-term degradation under physiological conditions, weak osseointegrative properties) [7-10], the original approach of its surface modification by a thin Ta/MWCNTs composite coating has proved to be highly beneficial and promising for applied perspectives [24,25]. Considering the achievements relative to the conversion treatment of carboxylic acids into bisphosphonic acids [50,51], and knowing the considerable affinity of the $–P(=O)(OH)_2$ groups for tantalum [42,43], we intend to check and evaluate the direct impact of the presence of these bisphosphonic functions closely attached to the nanotubes sidewalls. Experiments are carried out with four types of deposits: pristine Ta_2O_5, and composites Ta_2O_5/O-MWCNTs, Ta_2O_5/*weak* P-MWCNTs, and Ta_2O_5/*strong* P-MWCNTs. The first two situations, fully described in previous works [23-25,52], can be considered as reference cases compared to both kinds of P-MWCNTs-based deposits.

The surface chemical composition of the samples is assessed by XPS analyses. Fig. 4 presents the survey spectra of Ta_2O_5/*weak* P-MWCNTs and Ta_2O_5/*strong* P-MWCNTs composite coatings on Ti (a), as well as the respective core levels C1s (b), Ti2p (c) and Ta4f (d). The presence of tantalum in its oxidized form Ta_2O_5 is testified by the Ta4f doublet at 26.5 eV in both cases (Fig. 4d). The underlying Ti substrate is also detected through the representative

signal of Ti2p at 458.5-458.7 eV (Fig. 4c). Concerning the characterization of the detected carbon species, the analysis of the C1s peak (Fig. 4b) clearly highlights the presence of MWCNTs in the deposit, with a first peak at 284.3 eV attributed to the conjugated double bonds, and a second one at 293.1 eV corresponding to the π-π^* transitions in aromatic structures (satellite "shake-up" effect). Contributions for inherent atmospheric contaminations and residual oxidized functions (C=O, C(=O)O) on the CNTs sidewalls are also present. The evolution of Ta/Ti ratios for the four cases of Ta-based deposits is also particularly significant (Table 1): as previously noticed [24,25], a considerable increase of the Ta quantity on the Ti surface is observed between the pristine Ta_2O_5 layer (Ta/Ti = 0.90) and the three kinds of composite coatings (Ta/Ti ~ 3), with a slight improvement observed between the O-MWCNTs (Ta/Ti = 2.90) and the two cases – quite comparable – of P-MWCNTs (Ta/Ti = 3.2-3.3). Those trends confirm that the addition of MWCNTs in the sol-gel solution is highly beneficial for the precursor solution stability and the consolidation of the resulting tantalum oxide layer on the titanium surface. Moreover, this also suggests that matrices of strong C_{CNT}-P-O-Ta bonds are formed in solutions containing either *weak* or *strong* P-MWCNTs, which induces a reinforcement of the coating final quantity and stability. In this connection, the values obtained for the C_{sp2}/(Ti+Ta) ratios (with composite deposits) clearly point out the propensity of the phosphonic groups to "capture" tantalum: while O-MWCNTs lead to a C_{sp2}/(Ti+Ta) ratio of 0.53, P-MWCNTs result in lower values (0.21 for *weak* P-MWCNTs, 0.14 for *strong* P-MWCNTs), which indicates an inferior number of CNTs incorporated in the coating. This can be explained by a strengthening of the tantalum capture effect proportionally with the quantity of phosphonic functions present on the nanotubes sidewalls (as a reminder, they are higher on *strong* P-MWCNTs than on *weak* P-MWCNTs): the quicker and the stronger tantalum is captured by $-P(=O)(OH)_2$ groups (resulting in the increase of Ta/Ti ratio), the less time remains for CNTs to be incorporated in the deposit (resulting in the decrease of C_{sp2}/(Ti+Ta) ratio). In comparison with O-MWCNTs, the P-MWCNTs seem thus to get more benefits from the "tantalum capture effect" of their phosphonic moieties.

SEM images of the pristine and composite deposits allow a precise evaluation of their morphology and structure (Fig. 5). The pristine Ta_2O_5 coating (Fig. 5a) appears to be globally homogeneous and made of slightly fibrous nanostructures which can be well observed on the extremities of the occasional little cracks (insert in Fig. 5a). Concerning the three kinds of composite deposits, two situations are observed. For O-MWCNTs and *weak* P-MWCNTs (Fig. 5b and c), "spider web structures" of well-interlaced nanotubes are observed, with a strong homogeneous incorporation all over the layer. On the other hand, *strong* P-MWCNTs (Fig. 5d) remain intercompacted into "wool ball structures", which are noticed sporadically throughout the surface. The differences in the arrangement of the nanotubes in the deposits are directly related to the quality of their dispersion in the sol (constituted of absolute ethanol) during the formation step of the coatings. *Strong* P-MWCNTs are synthesized from strongly-oxidized MWCNTs (4 h at 60°C in H_2SO_4/HNO_3 3/1 v/v), which bare a more important number of oxidized groups on their sidewalls and should thus require more polar

solvents (e.g. water) to lead to better dispersion rates in the reaction solution, and further in the resulting deposits [41]. Weakly-oxidized MWCNTs (2 h at 50°C in H_2SO_4/HNO_3 3/1 v/v), used to prepare *weak* P-MWCNTs, are better solubilized in absolute ethanol and result thus in more homogeneous dispersions in the final coating.

Peeling tests are then processed on the four different kinds of coatings in order to qualitatively evaluate their adherent properties with respect to the substrate. As shown on Fig. 6, this aptitude is confirmed for all cases, given the fact that Ta-based layers are still observed after the scratching of the samples, with conservation of their respective morphological features (presence of nanotubes, “spider web” or “wool ball” structures, …).

The evaluation of the degree of wrapping of the MWCNTs by Ta_2O_5 when they are incorporated in the composite deposits is performed via TEM analyses. For this, Ta_2O_5/MWCNTs layers are first scratched from the Ti substrates with a spatula, then carefully dispersed in absolute ethanol, and a drop of the obtained suspension is finally deposited on a TEM grid for further characterization. TEM images of the different MWCNTs taken from the composite coatings are presented on Fig. 7. O-MWCNTs (Fig. 7a) and *strong* P-MWCNTs (Fig. 7c) appear clearly as a mixture of nude and slightly Ta_2O_5-covered (5 to 10 nm) carbon nanotubes. At the opposite, *weak* P-MWCNTs (Fig. 7b) remain strongly anchored in big metallic aggregates. The few nanotubes that bulge out of the extremities of the tantalum oxide blocks present a quite thick wrapping layer of Ta on their outer surface, going up to 20-30 nm, which is particularly remarkable. From these results, it looks like the (bis)phosphonic functionalization of the nanotubes has indeed a better ability to capture tantalum than simple oxidized groups, as shown by the tough increase of the wrapping from O-MWCNTs to *weak* P-MWCNTs. The weaker coverage by Ta_2O_5 noticed for *strong* P-MWCNTs is probably related to their poor solubilization capacities during the sol-gel process. This highlights again the great importance and predominance of the dispersion phenomenon for the preparation of CNTs-based composite materials.

3.3. *In vitro* growth of hydroxyapatite on Ta_2O_5/MWCNTs composite coatings on Ti

As final part of this study, the improvements brought by the modification of MWCNTs with bisphosphonic acid groups for their better incorporation into tantalum-based composite deposits on titanium are considered in perspective with the global bioactive skills of those materials. A qualitative and quantitative primary evaluation of these properties is accomplished by inducing the *in vitro* growth of a hydroxyapatite (HAp) $Ca_{10}(PO4)_6(OH)_2$ layer through the immersion of the samples in a simulated body fluid (SBF) solution. Thus Ti samples covered by pristine Ta_2O_5 and composites Ta_2O_5/O-MWCNTs, Ta_2O_5/*weak* P-MWCNTs, and Ta_2O_5/*strong* P-MWCNTs layers are placed for 7 days in 10 mL of the previously described SBF at 37°C and physiological pH of 7.25. The resulting HAp coatings are characterized by XPS and SEM/EDX.

XPS survey spectra of HAp layers covering Ta_2O_5/*weak* P-MWCNTs and Ta_2O_5/*strong* P-MWCNTs composite coatings on Ti are shown on Fig. 8. Characteristic peaks of the substrate (Ti2p), the deposit (C1s, Ta4f) and the hydroxyapatite film (Ca2p, P2p) are observed, combined with contaminations from the other constitutive elements of the SBF solution (K, Na, Cl, Mg). The presence of HAp is confirmed by the characteristic binding energies measured for Ca2p and P2p core levels (respectively 348.0 and 133.7 eV). Atomic ratios reported on Table 2 particularly point out the differences between the four kind of coating deposits. Ta_2O_5 pristine layers lead to relatively poor covering rates (Ca/(Ti+Ta) = 0.66 and P/(Ti+Ta) = 0.57) and to an experimental Ca/P ratio quite distant from the theoretical value (1.16 against 1.67, respectively). These ratios improve progressively with the introduction of O-MWCNTs in the deposits (Ca/(Ti+Ta) = 0.93, P/(Ti+Ta) = 0.73, Ca/P = 1.27), and even more with *weak* P-MWCNTs (Ca/(Ti+Ta) = 1.31, P/(Ti+Ta) = 1.00, Ca/P = 1.32). In a general way, this confirms that the incorporation of carbon nanotubes in the tantalum oxide matrix is likely to be beneficial for the primary osseous bioactivity of the material. Considering the specific presence of phosphonic functions on the nanotubes' sidewalls, it should be specified here that, although PO_3^{2-} moieties are also well known for their propensity to complex Ca^{2+} ions and favor the growth of HAp, they do not act directly in this way. Indeed they are not any more accessible from the interface with the external environment, considering the thick (20-30 nm) and homogeneous Ta layer covering the outer surface of CNTs. Thus the presence of bisphosphonic functions on P-MWCNTs, comparatively to O-MWCNTs, only act as positive factor on the intrinsic features of the tantalum-based composite deposit (higher quantity and compactness). The better results obtained with (*weak*) P-MWCNTs in terms of HAp growth are thus a consequence of the improvement of the tantalum "platform", and are not directly related to the CNTs functionalization. Finally, *strong* P-MWCNTs exhibit weaker characteristic ratios than the two other types of nanotubes, with numbers lying just above the pristine Ta_2O_5 case (Ca/(Ti+Ta) = 0.75, P/(Ti+Ta) = 0.65, Ca/P = 1.15). This should constitute an obvious indication that badly dispersed CNTs do not further lead to good morphological aptitudes in terms of bioactivity.

Concerning the SEM characterization of the HAp layers covering the four kinds of substrates (Fig. 9), large-scale images only testify for a substantial covering rate in each case. The relative number, form and size of HAp crystals are very heterogeneous and irregular all over the surface of a single substrate, and also from one sample to another. No significant particularities are thus noticed between the different examples. On more expanded views (Fig. 10a), observed HAp entities exhibit a kind of "gypsum flower" morphology. EDX analysis (Fig. 10b) confirms the chemical nature of the observed HAp crystals, with the appearance of strong contributions for Ca K and P K signals on the elemental mapping.

4. Conclusions

The successful incorporation of MWCNTs bearing phosphonic acid groups closely attached to their outer surface into tantalum-based coatings on titanium substrates has been achieved in this report. MWCNTs functionalized with bisphosphonic moeities from “weakly-oxidized” specimens have demonstrated strong abilities to induce the formation of substantial and rigid composite layers. They were homogeneously dispersed all over the deposits into “spider web structures”, and showed remarkably thick wrappings by tantalum oxide (up to 20-30 nm). By opposition, bisphosphonic-modified nanotubes prepared from “strongly-oxidized” specimens have shown poor dispersion capacities in the precursor solution made of absolute ethanol, which has resulted into a globally inhomogeneous insertion in the deposits under compact “wool ball structures”. They also present thinner coverings by tantalum oxide (5-10 nm). The fundamental importance of the good preliminary dispersion of the carbon nanotubes in the reaction solution during the sol-gel co-deposition process has thus been highlighted, as well as its crucial resulting impact on the *in vitro* hydroxyapatite growth capacities of the different surfaces. The so-prepared Ta_2O_5/*weak* P-MWCNTs composite coatings on Ti substrates constitute thus very interesting platforms in terms of qualitative osseous bioactivity, and can be considered for further research throughout orthopedic biomaterials topics.

Acknowledgment

A. Maho is grateful to FNRS-FRIA for fellowship.

References

[1] H.L. Freese, M.G. Volas, J.R. Wood, in D.M. Brunette, P. Tengval, M. Textor, P. Thomsen (Eds.), Titanium in Medicine, Springer-Verlag, Heidelberg, Germany, 2001, ch.3, pp. 25-51.

[2] M. Geetha, A.K. Singh, R. Asokamani, A.K. Gogia, Prog. Mater. Sci. 54 (2009) 397-425.

[3] M. Balazic, J. Kopac, M.J. Jackson, W. Ahmed, Int. J. Nano. Biomater. 1 (2007) 3-34.

[4] C.N. Elias, J.H.C. Lima, R. Valiev, M.A. Meyers, JOM J. Min. Met. Mat. S. 60 (2008) 46-49.

[5] J. Pouilleau, D. Devilliers, F. Garrido, S. Durand-Vidal, E. Mahé, Mater. Sci. Eng. B 47 (1997) 235-243.

[6] N. Tran, T.J. Webster, Wiley Interdiscip. Rev. Nanomed. Nanobiotechnol. 1 (2009) 336-351.

[7] D. Krupa, J. Baszkiewicz, J.W. Sobczak, A. Bilinski, A. Barcz, J. Mater. Process. Technol. 143-144 (2003) 158-163.

[8] D. Krupa, J. Basekiewicz, J.A. Kozubowski, J. Mizera, A. Barcz, J.W. Sobczak, A. Bilinski, B. Rajchel, Anal. Bioanal. Chem. 381 (2005) 617-625.

[9] D. Zaffe, C. Bertoldi, U. Consolo, Biomaterials 24 (2003) 1093-1099.

[10] Y. Nuevo-Ordonez, M. Montes-Bayon, E. Blanco-Gonzalez, J. Paz-Aparicio, J. Dianez Raimundez, J.M. Tejerina, M.A. Pena, A. Sanz-Medel, Anal. Bioanal. Chem. 401 (2011) 2747-2754.

[11] S.A. Shabalovskaya, BioMed. Mater. Eng. 6 (1996) 267-289.

[12] Y. Okazaki, E. Gotoh, Biomaterials 26 (2005) 11-21.

[13] J. Black, Clin. Mater. 16 (1994) 167-173.

[14] T. Miyazaki, H.-M. Kim, T. Kokubo, C. Ohtsuki, H. Kato, T. Nakamura, Biomaterials, 23 (2002) 827-832.

[15] M.-D. Bermudez, F.J. Carrion, G. Martinez-Nicolas, R. Lopez, Wear 258 (2005) 693-700.

[16] D.C.N. Chan, H.W. Titus, K.-H. Chung, H. Dixon, S.T. Wellinghoff, H.R. Rawls, Dent. Mater. 15 (1999) 219-222.

[17] P.J.F. Harris, Int. Mater. Rev. 49 (2004) 31-43.

[18] S. Sirivisoot, T.J. Webster, Nanotechnology 19 (2008) 295101/1-12.

[19] S. Liao, G. Xu, W. Wang, F. Watari, F. Cui, S. Ramakrishna, C.K. Chan, Acta Biomater. 3 (2007) 669-675.

[20] C.J. Brinker, G.W. Scherer, in Sol-gel science: the physics and chemistry of sol-gel processing, Academic Press, San Diego, USA, 1990, ch. 2, pp. 21-95.

[21] N.P. Bansal, J. Mater. Sci. 29 (1994) 5065-5070.

[22] C. Chaneliere, J.L. Autran, R.A.B. Devine, B. Balland, Mater. Sci. Eng. R 22 (1998) 269-322.

[23] C. Arnould, C. Volcke, C. Lamarque, P.A. Thiry, J. Delhalle, Z. Mekhalif, J. Colloid. Interface Sci. 336 (2009) 497-503.

[24] C. Arnould, T.J. Koranyi, J. Delhalle, Z. Mekhalif, J. Colloid. Interface Sci. 344 (2010) 390-394.

[25] A. Maho, S. Linden, C. Arnould, S. Detriche, J. Delhalle, Z. Mekhalif, J. Colloid. Interface Sci. 371 (2012) 150-158.

[26] J.-C. Ma, W.-D. Zhang, Microchim. Acta 175 (2011) 309-314.

[27] F. Tan, X. Fan, G. Zhang, F. Zhang, Mater. Lett. 61 (2007) 1805-1808.

[28] Y. Liu, W. Jiang, S. Li, F. Li, Appl. Surf. Sci. 255 (2009) 7999-8002.

[29] B. Gao, G.Z. Chen, G.L. Puma, Appl. Catal. B 89 (2009) 503-509.

[30] P. Martis, B.R. Venugopal, J.-S. Seffer, J. Delhalle, Z. Mekhalif, Acta Mater. 59 (2011) 5040-5047.

[31] P. Martis, B.R. Venugopal, J. Delhalle, Z. Mekhalif, J. Solid State Chem. 184 (2011) 1245-1250.

[32] C.M. Hansen, in Hansen solubility parameters: a user's handbook, CRC Press, Boca Raton, USA, 2000, pp. 1-24.

[33] S. Detriche, G. Zorzini, J.-F. Colomer, A. Fonseca, J. B.Nagy, J. Nanosci. Nanotechnol. 8 (2008) 1-11.

[34] D. Tasis, N. Tagmatarchis, A. Bianco, M. Prato, Chem. Rev. 106 (2006) 1105-1136.

[35] D. Eder, Chem. Rev. 110 (2010) 1348-1385.

[36] X.-B. Yan, B.K. Tay, Y. Yang, J. Phys. Chem. B 110 (2006) 25844-25849.

[37] Y.-P. Sun, K. Fu, Y. Lin, W. Huang, Acc. Chem. Res. 35 (2002) 1096-1104.

[38] K.J. Ziegler, Z. Gu, H. Peng, E.L. Flor, R.H. Hauge, R.E. Smalley, J. Am. Chem. Soc. 127 (2005) 1541-1547.

[39] V. Datsyuk, M. Kalyva, K. Papagelis, J. Parthenios, D. Tasis, A. Siokou, I. Kallitsis, and C. Galiotis, Carbon 46 (2008) 833-840.

[40] Y. Xiao, T. Gong, S. Zhou, Biomaterials 31 (2010) 5182-5190.

[41] S. Detriche, J. B.Nagy, Z. Mekhalif, J. Delhalle, J. Nanosci. Nanotechnol. 9 (2009) 1-11.

[42] D. Brovelli, G. Hähner, L. Ruiz, R. Hofer, G. Kraus, A. Waldner, J. Schlösser, P. Oroszlan, M. Ehrat, N.D. Spencer, Langmuir 15 (1999) 4324-4327.

[43] E. Jaehne, S. Oberoi, H.-J.P. Adler, Prog. Org. Coat. 61 (2008) 211-223.

[44] C.S. Demmer, N. Krogsgaard-Larsen, L. Bunch, Chem. Rev. 111 (2011) 7981-8006.

[45] H. Fleisch, Breast Cancer Res. 4 (2002) 30-34.

[46] R.G.G. Russell, N.B. Watts, F.H. Ebetino, M.J. Rogers, Osteoporos. Int. 19 (2008) 733-759.

[47] T. Sainsbury, D. Fitzmaurice, Chem. Mater. 16 (2004) 3780-3790.

[48] B. Zhao, H. Hu, S.K. Mandal, R.C. Haddon, Chem. Mater. 17 (2005) 3235-3241.

[49] A. Oki, L. Adams, V. Khabashesku, Y. Edigin, P. Biney, Z. Luo, Mater. Lett. 62 (2008) 918-922.

[50] M. Lecouvey, I. Mallard, T. Bailly, R. Burgada, Y. Leroux, Tetrahedron Lett. 42 (2001) 8475-8478.

[51] G. Lecollinet, N. Delorme, M. Edely, A. Gibaud, J.-F. Bardeau, F. Hindré, F. Boury, D. Portet, Langmuir 25 (2009) 7828-7835.

[52] C. Arnould, J. Denayer, M. Planckaert, J. Delhalle, Z. Mekhalif, J. Colloid. Interface Sci. 341 (2010) 75-82.

[53] S.V. Kononova, M.A. Nesmeyanova, Biochemistry (Moscow) 67 (2002) 184-195.

Figure captions

Fig. 1. Synthesis protocols of *weak* P-MWCNTs (up) and *strong* P-MWCNTs (down) from crude multiwalled carbon nanotubes (MWNT 7000, Nanocyl).

Fig. 2. Principles of the sol-gel processes: (a) sol-gel deposition of Ta_2O_5 on Ti, (b) sol-gel co-deposition of Ta_2O_5 and MWCNTs on Ti.

Fig. 3. XPS survey spectra of (a) *weak* P-MWCNTs and (b) *strong* P-MWCNTs.

Fig. 4. XPS survey spectra (a) and core levels of C1s (b), Ti2p (c) and Ta4f (d) of composite coatings of Ta_2O_5 and *weak* P-MWCNTs (up) and *strong* P-MWCNTs (down) generated on Ti.

Fig. 5. SEM pictures of Ti substrates covered by (a) pristine Ta_2O_5 (insert: magnified view) and composite (b) Ta_2O_5/O-MWCNTs, (c) Ta_2O_5/*weak* P-MWCNTs, and (d) Ta_2O_5/*strong* P-MWCNTs coatings.

Fig. 6. SEM pictures after peeling tests of Ti substrates covered by (a) pristine Ta_2O_5 and composite (b) Ta_2O_5/O-MWCNTs, (c) Ta_2O_5/*weak* P-MWCNTs, and (d) Ta_2O_5/*strong* P-MWCNTs coatings.

Fig. 7. TEM pictures of (a) O-MWCNTs, (b) *weak* P-MWCNTs, and (c) *strong* P-MWCNTs after their extraction from the respective Ta_2O_5-based composite deposits on Ti.

Fig. 8. XPS survey spectra of hydroxyapatite films on Ti substrates covered by composite layers of Ta_2O_5 and (a) *weak* P-MWCNTs and (b) *strong* P-MWCNTs.

Fig. 9. SEM pictures of hydroxyapatite deposited on Ti substrates covered by (a) pristine Ta_2O_5 and composite (b) Ta_2O_5/O-MWCNTs, (c) Ta_2O_5/*weak* P-MWCNTs, and (d) Ta_2O_5/*strong* P-MWCNTs coatings.

Fig. 10. (a) SEM picture (enlarged view) of a representative hydroxyapatite crystal deposited on the tantalum-based surfaces, and (b) corresponding EDX analysis with Na K, P K, Cl K, Ca K, Ti K, and Ta M signals.

Figures

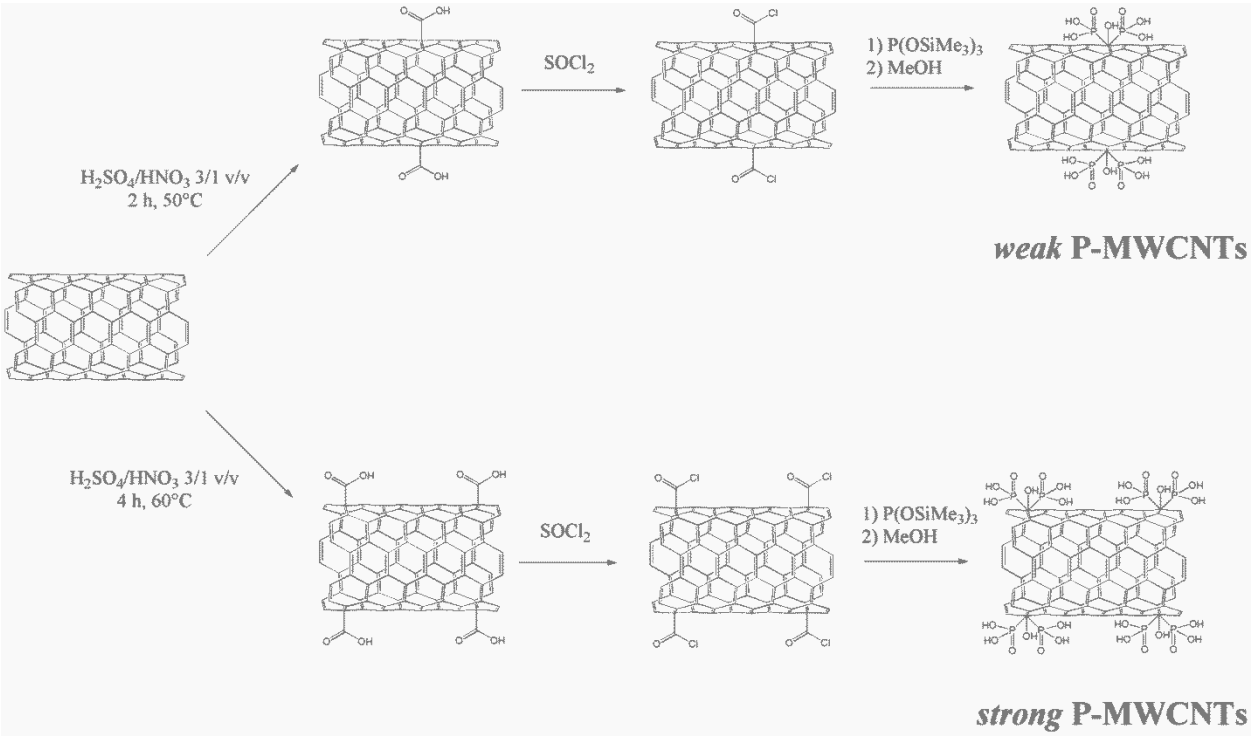

Fig. 1. Synthesis protocols of *weak* P-MWCNTs (up) and *strong* P-MWCNTs (down) from crude multiwalled carbon nanotubes (MWNT 7000, Nanocyl).

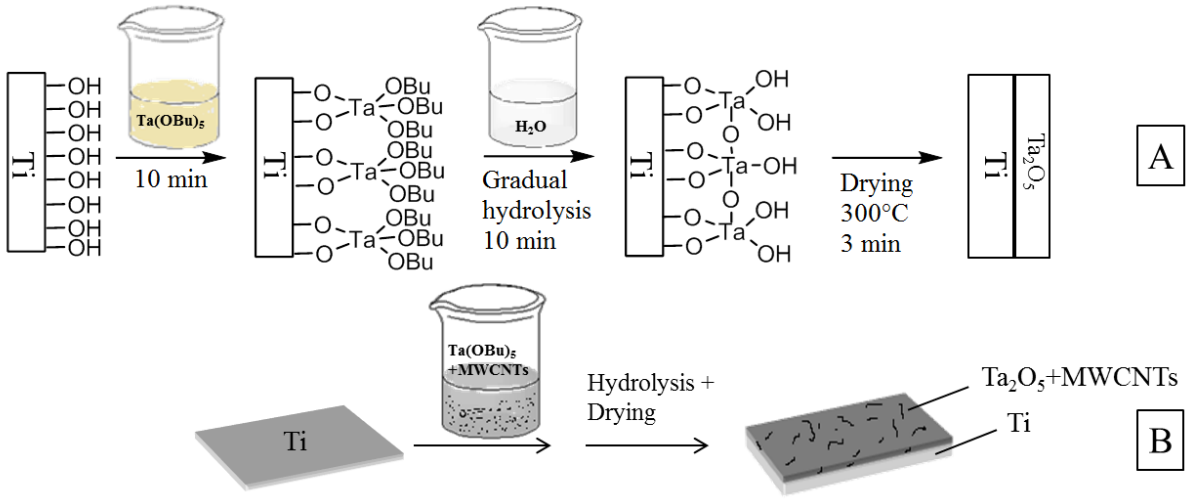

Fig. 2. Principles of the sol-gel processes: (a) sol-gel deposition of Ta_2O_5 on Ti, (b) sol-gel co-deposition of Ta_2O_5 and MWCNTs on Ti.

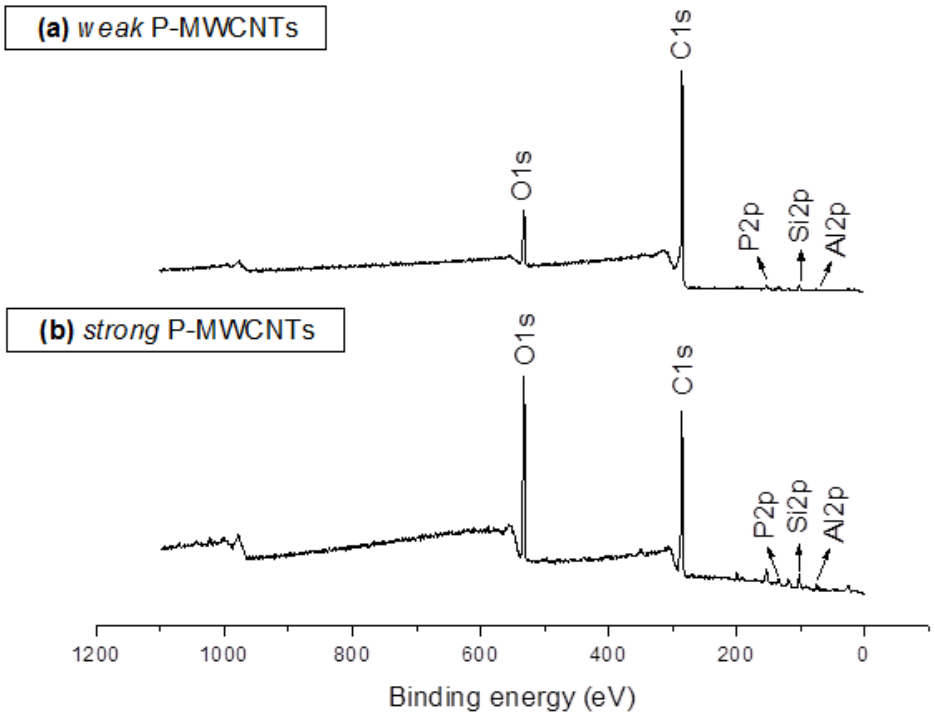

Fig. 3. XPS survey spectra of (a) *weak* P-MWCNTs and (b) *strong* P-MWCNTs.

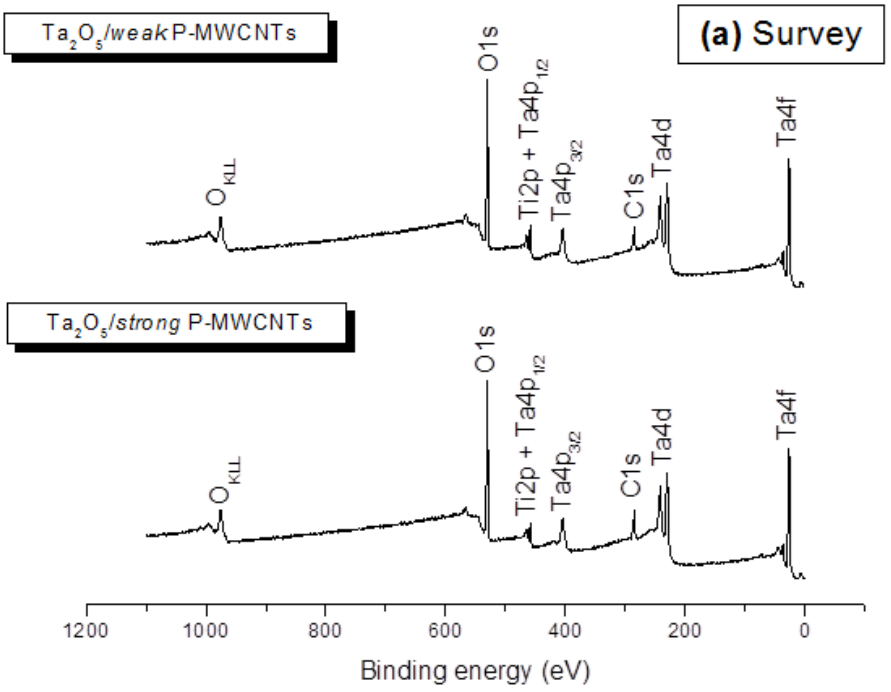
Ta2O5/weak P-MWCNTs
(a) Survey
O1s
Ti2p + Ta4p1/2
Ta4p3/2
C1s
Ta4d
Ta4f
OKLL
Ta2O5/strong P-MWCNTs
1200
1000
800
600
400
200
0
Binding energy (eV)

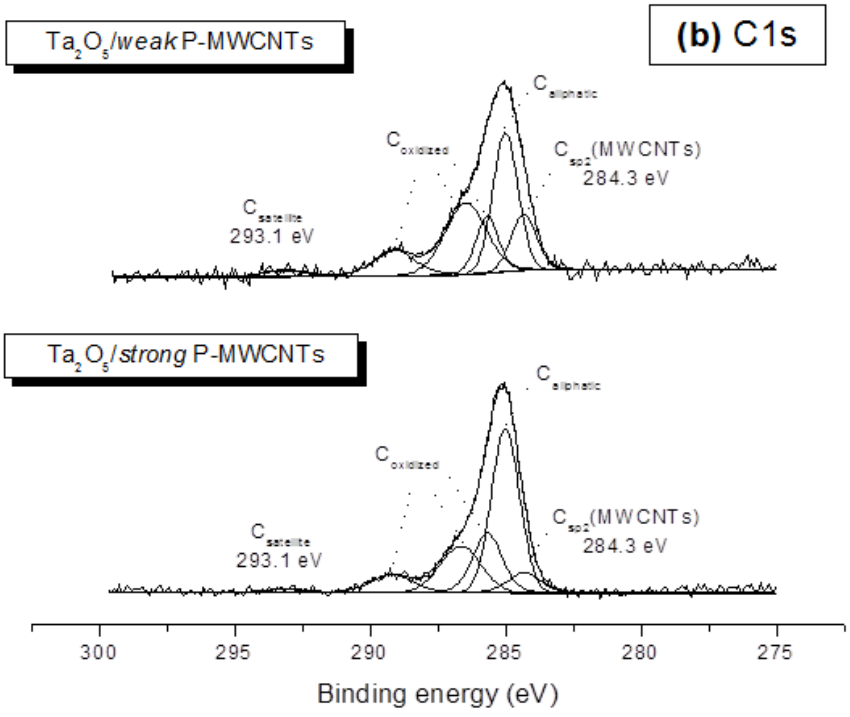
Ta2O5/weak P-MWCNTs
(b) C1s
Caliphatic
Coxidized
Csp2(MWCNTs)
284.3 eV
Csatellite
293.1 eV
Ta2O5/strong P-MWCNTs
300
295
290
285
280
275
Binding energy (eV)

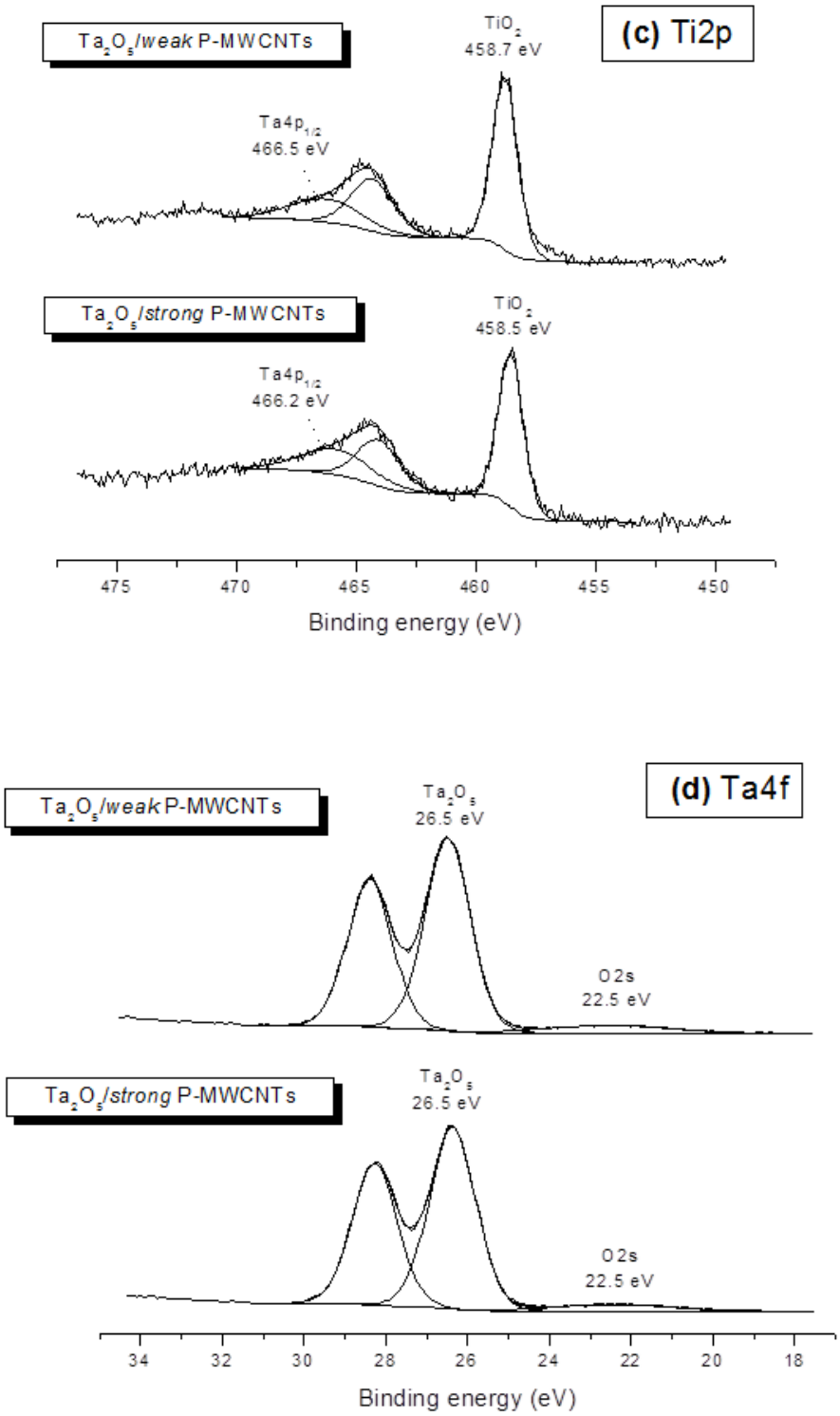

Fig. 4. XPS survey spectra (a) and core levels of C1s (b), Ti2p (c) and Ta4f (d) of composite coatings of Ta_2O_5 and *weak* P-MWCNTs (up) and *strong* P-MWCNTs (down) generated on Ti.

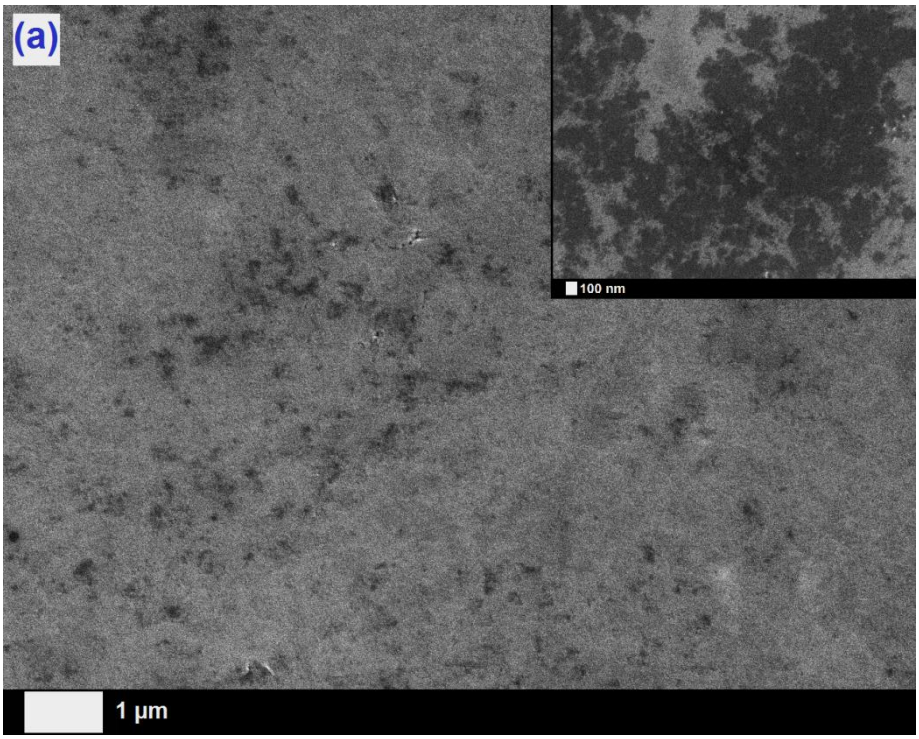
(a)
100 nm
1 µm

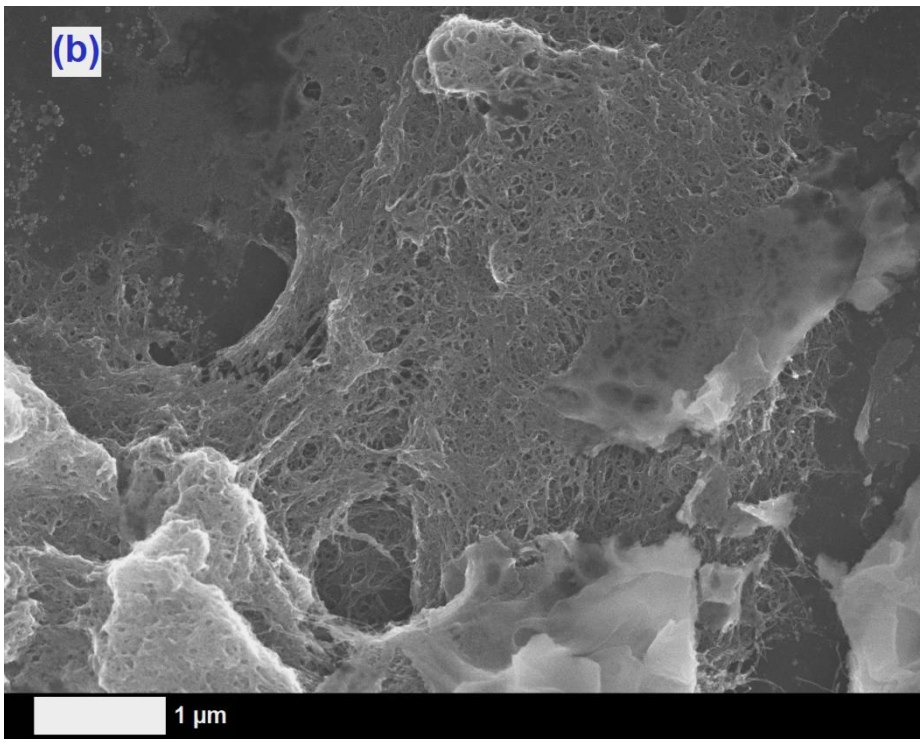
(b)
1 µm

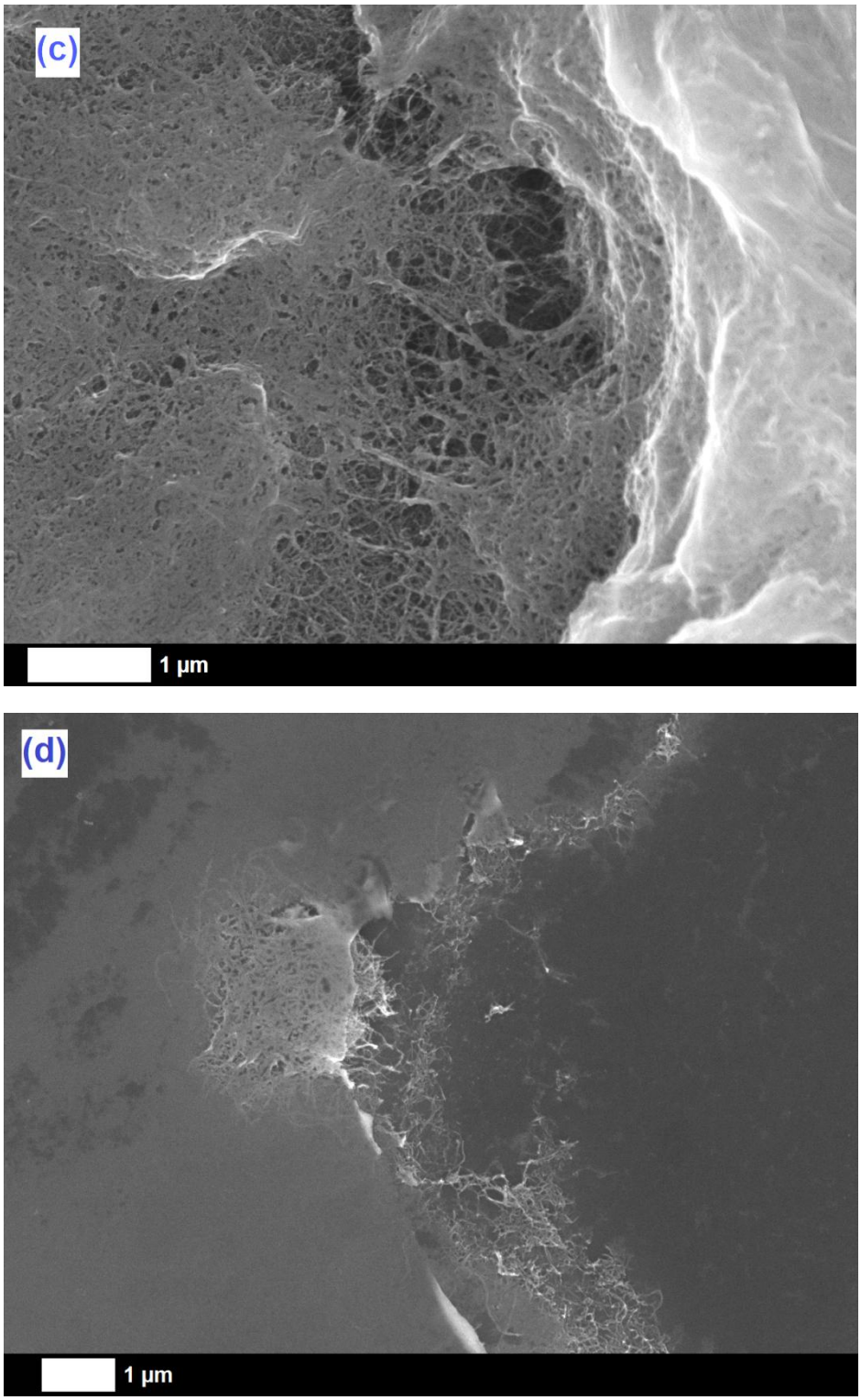

Fig. 5. SEM pictures of Ti substrates covered by (a) pristine Ta_2O_5 (insert: magnified view) and composite (b) Ta_2O_5/O-MWCNTs, (c) Ta_2O_5/*weak* P-MWCNTs, and (d) Ta_2O_5/*strong* P-MWCNTs coatings.

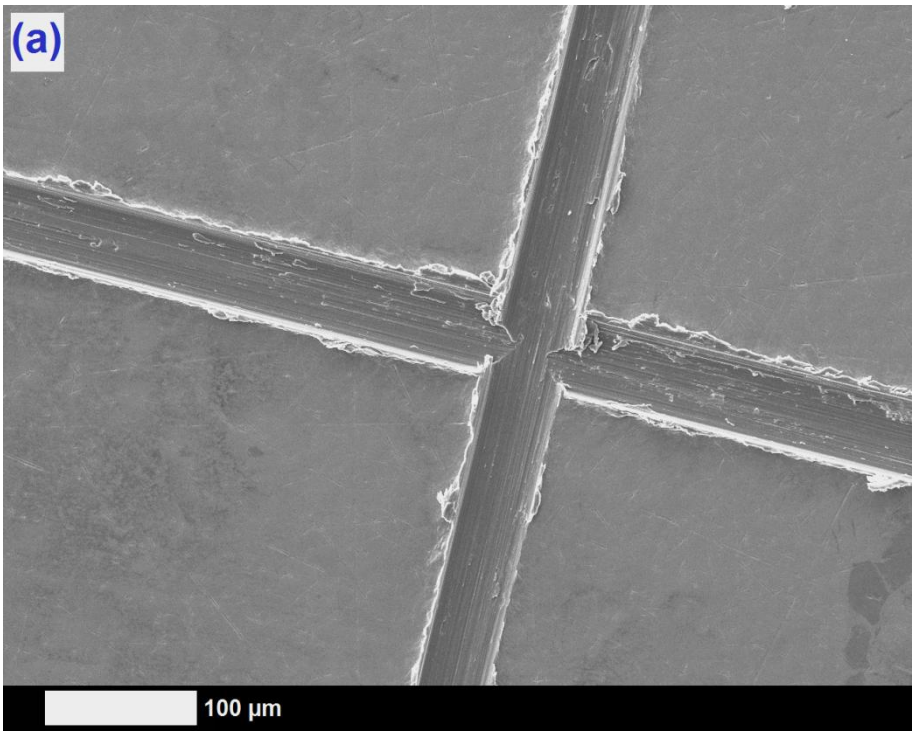
(a)
100 µm

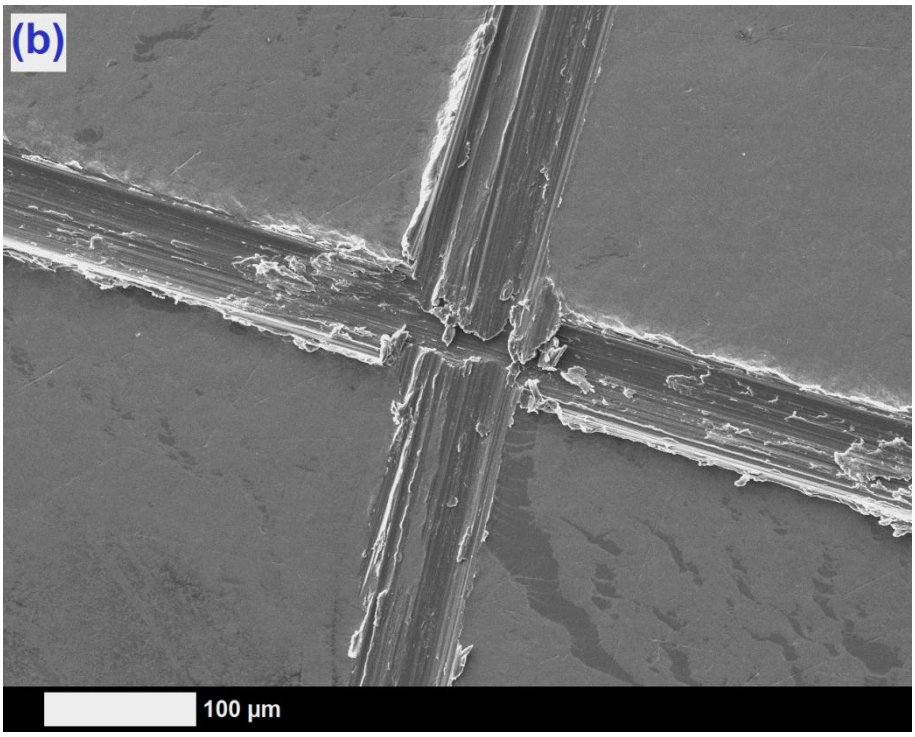
(b)
100 µm

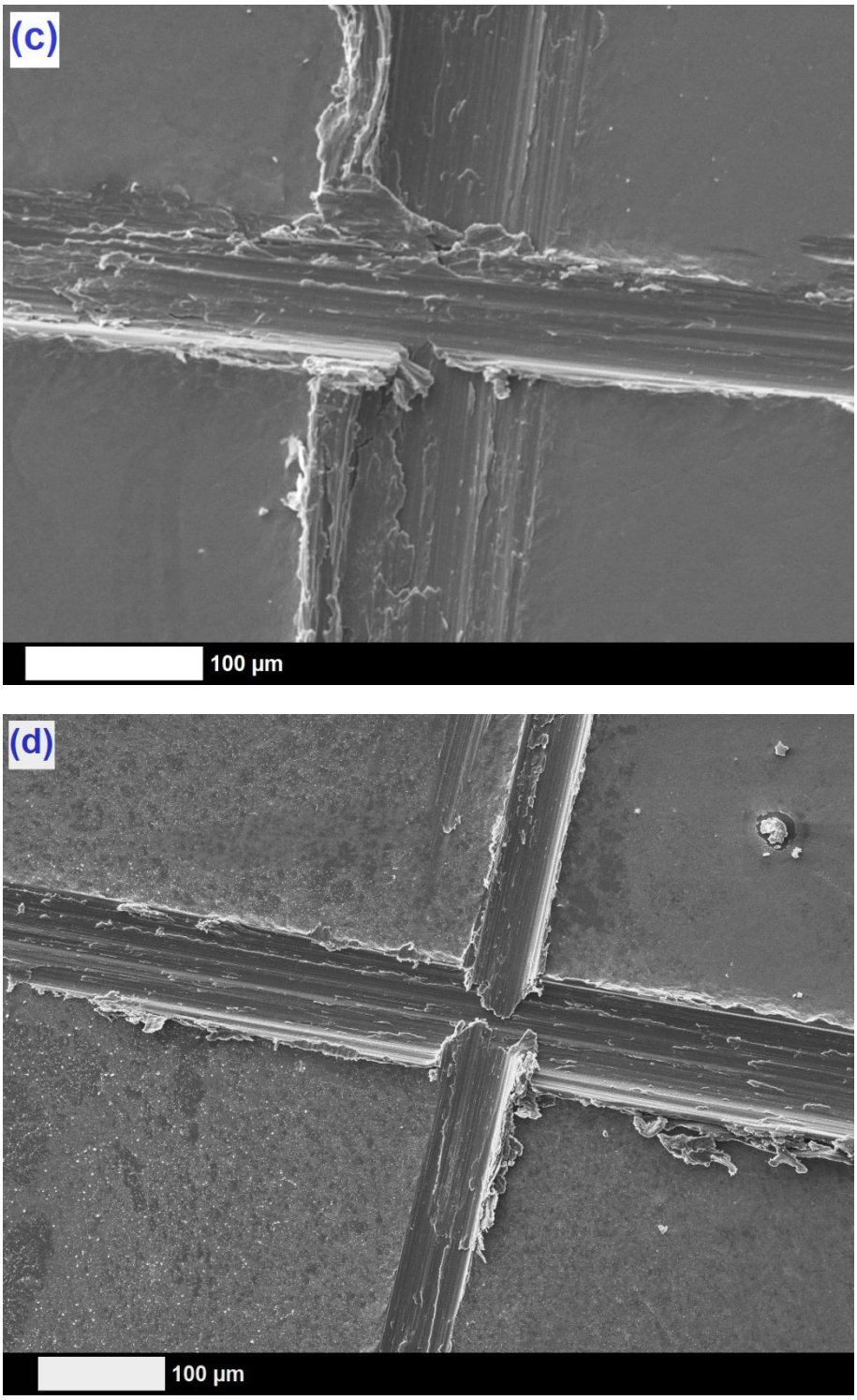

Fig. 6. SEM pictures after peeling tests of Ti substrates covered by (a) pristine Ta_2O_5 and composite (b) Ta_2O_5/O-MWCNTs, (c) Ta_2O_5/*weak* P-MWCNTs, and (d) Ta_2O_5/*strong* P-MWCNTs coatings.

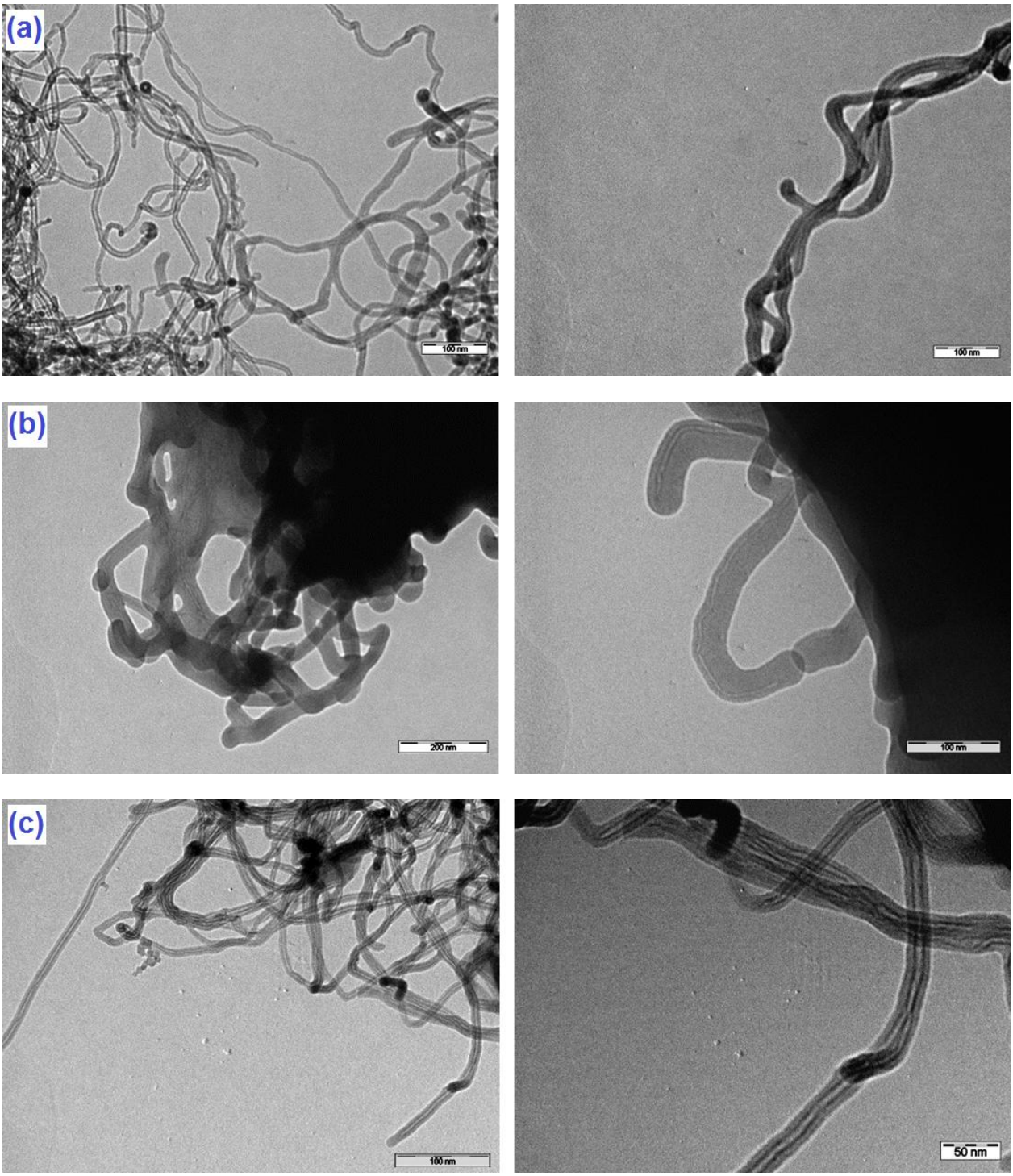

Fig. 7. TEM pictures of (a) O-MWCNTs, (b) *weak* P-MWCNTs, and (c) *strong* P-MWCNTs after their extraction from the respective Ta_2O_5-based composite deposits on Ti.

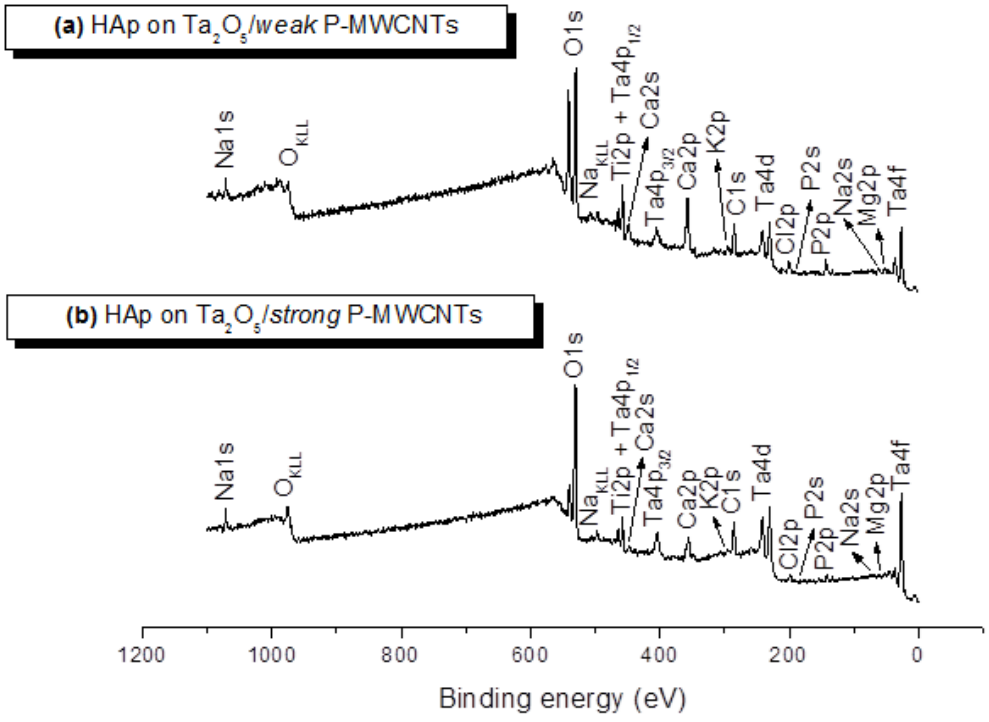

Fig. 8. XPS survey spectra of hydroxyapatite films on Ti substrates covered by composite layers of Ta_2O_5 and (a) *weak* P-MWCNTs and (b) *strong* P-MWCNTs.

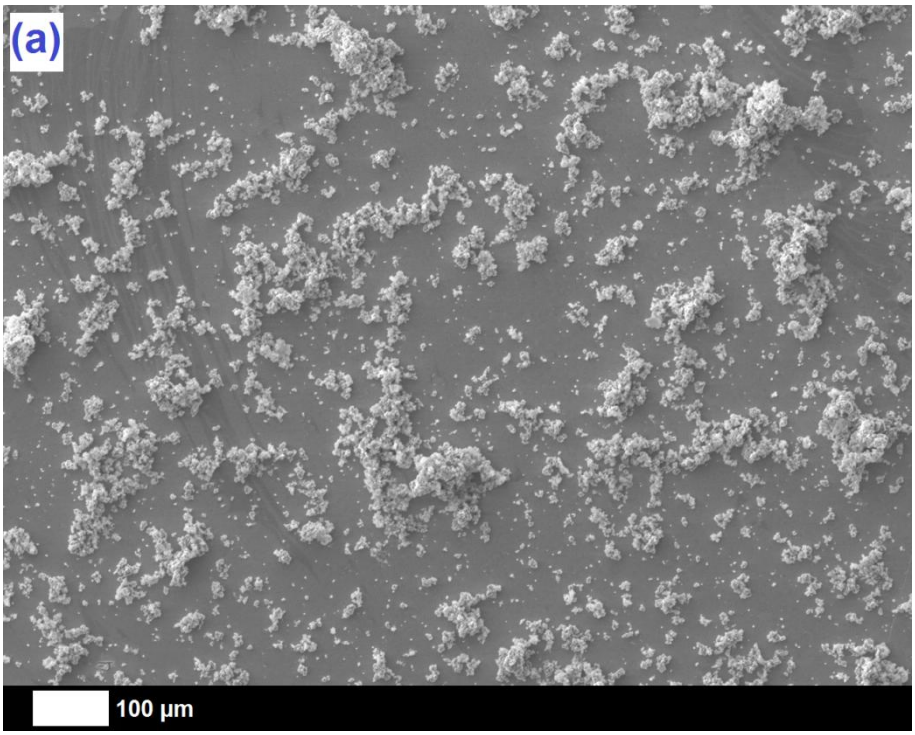
(a)
100 µm

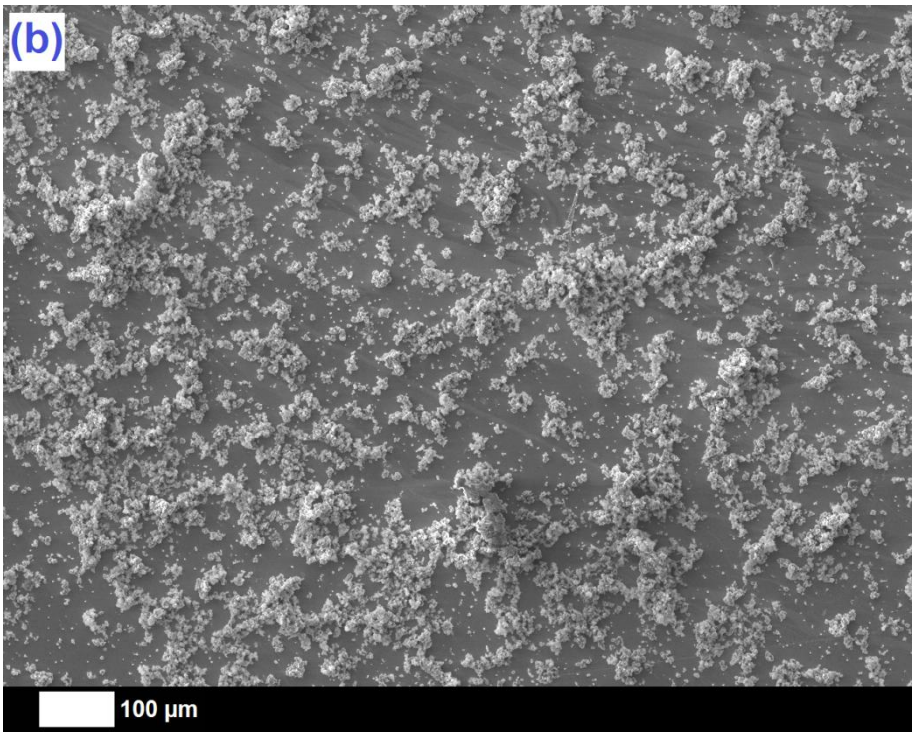
(b)
100 µm

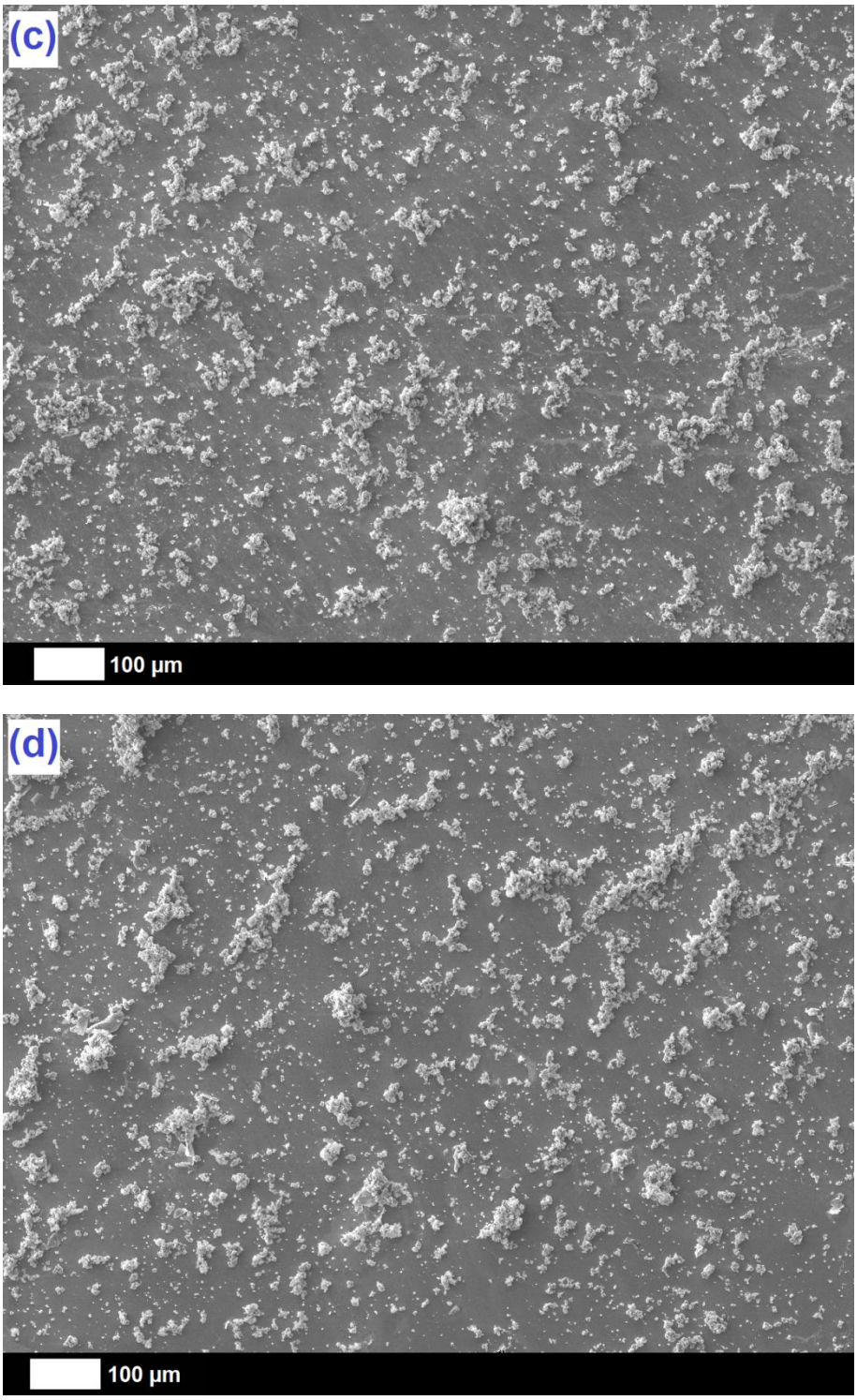

Fig. 9. SEM pictures of hydroxyapatite deposited on Ti substrates covered by (a) pristine Ta_2O_5 and composite (b) Ta_2O_5/O-MWCNTs, (c) Ta_2O_5/*weak* P-MWCNTs, and (d) Ta_2O_5/*strong* P-MWCNTs coatings.

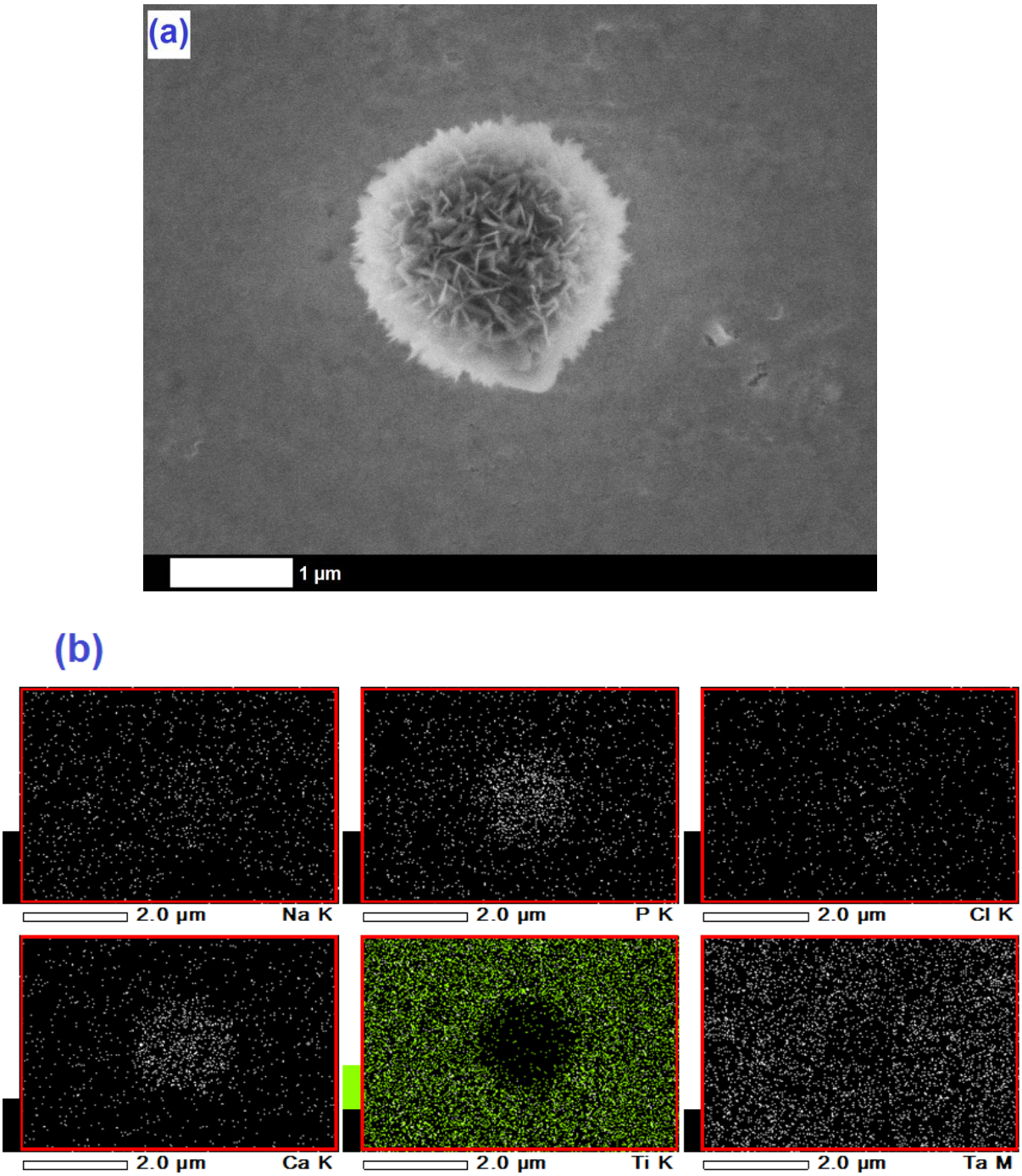

Fig. 10. (a) SEM picture (enlarged view) of a representative hydroxyapatite crystal deposited on the tantalum-based surfaces, and (b) corresponding EDX analysis with Na K, P K, Cl K, Ca K, Ti K, and Ta M signals.

Tables

Table 1. XPS Ta/Ti and C_{sp2}/(Ti+Ta) ratios for tantalum-based layers deposited on Ti surfaces by sol-gel deposition

Deposit	Ta/Ti	C_{sp2}/(Ti+Ta)
Pristine Ta_2O_5	0.90	//
Composite Ta_2O_5/O-MWCNTs	2.90	0.54
Composite Ta_2O_5/*weak* P-MWCNTs	3.29	0.21
Composite Ta_2O_5/*strong* P-MWCNTs	3.22	0.14

Table 2. XPS Ca/(Ti+Ta), P/(Ti+Ta) and Ca/P ratios for hydroxyapatite films formed on tantalum-based layers deposited on Ti surfaces

Deposit	Ca/(Ti+Ta)	P/(Ti+Ta)	Ca/P
Pristine Ta_2O_5	0.66	0.57	1.16
Composite Ta_2O_5/O-MWCNTs	0.93	0.73	1.27
Composite Ta_2O_5/*weak* P-MWCNTs	1.31	1.00	1.32
Composite Ta_2O_5/*strong* P-MWCNTs	0.75	0.75	1.15